4-20-2010

Magnetoelasticity of Fe–Si single crystals

Qingfeng Xing
Iowa State University, qxing@ameslab.gov

D. Wu
Iowa State University

Thomas A. Lograsso
Iowa State University, lograsso@ameslab.gov

Magnetoelasticity of Fe–Si single crystals

Abstract
The tetragonal magnetostriction constant, $(3/2)\lambda_{100}$, of Fe–Si single crystals was measured and was found to be structure dependent. Similar to that of Fe–Ge single crystals, $(3/2)\lambda_{100}$ is positive in the single phase A2 regime, becomes negative in the single phase $D0_3$ regime, and changes from positive to negative between the two regimes. Short-range order in the A2 regime decreases the magnetostriction prior to the onset of long range order. In the single phase regions of both A2 and $D0_3$, thermal history does not show any obvious effect on the magnetostriction, contrary to that found for Fe–Ga alloys. However, in the regions of phase mixture involving A2, B2, and $D0_3$ phases, quenching pushes the change in magnetostriction from positive to negative to higher Si contents.

Keywords
iron alloys, magnetostriction, short-range order, silicon alloys

Disciplines
Condensed Matter Physics | Metallurgy

The following article appeared in *Journal of Applied Physics* 107 (2010): 09A911 and may be found at http://dx.doi.org/10.1063/1.3353017.

AIP | Journal of Applied Physics

Magnetoelasticity of Fe–Si single crystals

Q. Xing, D. Wu, and T. A. Lograsso

Citation: J. Appl. Phys. **107**, 09A911 (2010); doi: 10.1063/1.3353017
View online: http://dx.doi.org/10.1063/1.3353017
View Table of Contents: http://jap.aip.org/resource/1/JAPIAU/v107/i9
Published by the AIP Publishing LLC.

Magnetoelasticity of Fe–Si single crystals

Q. Xing (邢庆峰),[a] D. Wu, and T. A. Lograsso
Division of Materials Sciences and Engineering, Ames Laboratory, Ames, Iowa 50011, USA

(Presented 19 January 2010; received 24 October 2009; accepted 7 December 2009; published online 20 April 2010)

The tetragonal magnetostriction constant, $(3/2)\lambda_{100}$, of Fe–Si single crystals was measured and was found to be structure dependent. Similar to that of Fe–Ge single crystals, $(3/2)\lambda_{100}$ is positive in the single phase A2 regime, becomes negative in the single phase $D0_3$ regime, and changes from positive to negative between the two regimes. Short-range order in the A2 regime decreases the magnetostriction prior to the onset of long range order. In the single phase regions of both A2 and $D0_3$, thermal history does not show any obvious effect on the magnetostriction, contrary to that found for Fe–Ga alloys. However, in the regions of phase mixture involving A2, B2, and $D0_3$ phases, quenching pushes the change in magnetostriction from positive to negative to higher Si contents. © *2010 American Institute of Physics*. [doi:10.1063/1.3353017]

I. INTRODUCTION

Fe–Ga alloys received extensive attention over the past decade since the discovery of their attractive combination of magnetostrictive and mechanical properties. These alloys exhibit a strong dependence of the tetragonal magnetostriction constant, $(3/2)\lambda_{100}$, on the distribution of phases. The large magnetostriction boosted the research interests to other Fe-based binary alloys to understand the origins of the magnetoelastic enhancement. The magnetoelastic behavior of Fe–Ga single crystals has been categorized into four distinct magnetostriction-composition regimes.[1] In regime I with disordered single phase A2 and regime III with well ordered single phase $D0_3$, $(3/2)\lambda_{100}$ increases with Ga content, reaching a maximum of about 390 ppm around 20.6 at. % Ga for I and 440 ppm at 28.5 at. % Ga for III. These maximums correspond to the solubility limits of these single phase regions. In regimes II and IV, two-phase mixtures of A2 $+D0_3$ and $D0_3+$secondary phases, respectively, are found to exist and the phase distribution is known to be thermal history dependent.[1] It has been shown that $D0_3$ phase and regions of small secondary phases do not influence the distribution of the magnetic domains in the alloys, unless the secondary phases at higher Ga content are pronounced and large in size.[2] A corresponding variation of the rhombohedral magnetostriction constant, $(3/2)\lambda_{111}$, is also found over the same concentration range.[3]

Fe–Al alloys exhibit only two regimes: $(3/2)\lambda_{100}$ increases with Al contents up to ~16.6 at. % Al with a maximum of about 193 ppm and decreases to ~25 ppm at ~29 at. % Al.[4] In a previous report,[5] the magnetoelastic behavior of Fe–Al alloys shows only a qualitative dependence of thermal processing. The extensive studies of the alloys (e.g., see Ref. 6) show that the first regime corresponds to single phase A2 and the second regime to a phase mixture of $A2+D0_3$, and single phase $D0_3$. For Fe–Al alloys, the composition of the A2-$D0_3$ phase boundary is also dependent on thermal treatment.[6] The Curie temperature of the $D0_3$ phase drops rapidly with Al content, down to 200 °C at ~30 at. % Al.[6] This is believed to correspond to the low magnetostriction of the $D0_3$ phase and consequently to the absence of the two maxima behavior observed in Fe–Ga alloys.

Single crystals of Fe–Ge exhibit three magnetostriction-composition regimes.[7] In the first regime (up to ~10 at. % Ge), $(3/2)\lambda_{100}$ increases with Ge additions, reaching a maximum of 94 ppm at the solubility limit of the disordered A2 phase. Higher Ge contents between ~12 and 16 at. % Ge (within the $A2+D0_3$ two-phase region), result in decreases in magnetostriction which changes from positive to negative strains. For Ge contents with higher than 16 at. %, the magnetostriction remains negative with an absolute value of strain of 129 ppm at 18 at. % Ge. Thermal history has little influence on the magnetoelasticity of Fe–Ge alloys.[8]

The magnetoelasticity of Fe–Si is less understood than that of the above alloys. Initial work on Fe–Si was carried out by Carr *et al.*[9] and Hall[5] up to ~15 at. % Si. Their results show a sign change in $(3/2)\lambda_{100}$ from positive to negative strains with increasing Si content. The sign change is similar to what has been found in Fe–Ge.[6] In this work, we examine the single crystalline magnetostriction of Fe–Si over a wider range of Si compositions and investigate the effect of thermal processing on $(3/2)\lambda_{100}$. Magnetoelastic coupling factors are calculated using published elastic moduli experimental data. Comparisons are made to other Fe-based alloys.

II. EXPERIMENTAL

Fe–Si single crystals were grown by Bridgman technique,[7] followed by a homogenizing anneal at 1000 °C for one week in an Ar atmosphere. The samples were then cooled from 1000 °C at 10 °C/min (slow cooling). Disks for magnetostriction measurements that had a diameter of 6.35 mm and a thickness of 2.5 mm were cut from the samples. The disk plane was oriented along (100) plane by back Laue x-ray diffraction (XRD). Sample composition of individual disks was determined by electron probe microanalysis, using pure iron and silicon standards for calibra-

[a]Author to whom correspondence should be addressed. Tel.: +1 515 294 4693. Electronic mail: qxing@ameslab.gov.

tion. After the initial magnetostriction measurement, some disks were sealed in quartz tubes under an Ar atmosphere and subsequently annealed at 1000 °C for 4 h and quenched into ice-water, and measured again. The quenching process induced cracks within some samples, but the cracked samples still had regions that were crack-free and large enough for mounting strain gauges.

Magnetostriction measurements were carried out using the standard strain gauge method in a 20 kOe uniform magnetic field. The field was produced by electromagnets and was measured via a Hall probe. Appling the field parallel or perpendicular to a strain gauge glued onto an aluminum dummy sample produced no measurable magnetoresistance in the gauge. Three-wire gauge setup in a Wheatstone bridge was employed for temperature compensation. Magnetization measurements showed that 20 kOe is well above the field necessary to saturate the single crystals. Samples were initially mounted to make the gauge direction approximately perpendicular to the field direction and were rotated around their disk axes during the measurements. The field was applied in the (100) disk plane. $(3/2)\lambda_{100}$ was extracted by least-squares fit of the strain-angle data with an angular expression, $-(3/2)\lambda_{100}^{*}\cos^2(\theta+\alpha)+c$, where θ is the readout angle from the motor for sample rotation, α is the difference between the readout angle and the angle between the magnetic field and the measured direction and is a variable for fitting ($\theta+\alpha$ denotes the angle between the magnetic field and measured direction), and c is a constant which has contributions from both the magnetostriction and the balance point of the strain gauge bridge.

Structural characterization was carried out on the sample disks using XRD in a Bragg–Brentano geometry and copper Kα radiation. The samples were subjected to a deep Nital etch to remove any surface damage layer. Scattering was done in the (100) sample plane and the samples were rotated around the [100] axis at 60 rpm during the measurement.

III. RESULTS AND DISCUSSIONS

The dependence of $(3/2)\lambda_{100}$ on Si content is shown in Fig. 1 and is in good agreement with previous work[5,9,10] in the overall compositional dependence and in the effect of sample cooling rate from high-temperature anneals on $(3/2)\lambda_{100}$. However, the current values for Fe-3 at. % Si and Fe-5 at. % Si are up to ~40% larger than those reported in the previous work. This discrepancy is likely to come from a form factor[11] which we did not take into account. We are working on the correction by the form factor. Similar to the dependence in Fe–Ge single crystals,[7] $(3/2)\lambda_{100}$ increases with Si content up to ~5 at. %, then decreases across zero to negative values. Between 10 and 13 at. % Si, ice-water quenching shifts the change in $(3/2)\lambda_{100}$ from positive to negative to higher Si concentrations. For other compositions, thermal processing does not have a large effect on $(3/2)\lambda_{100}$. Between 5 and 13 at. % Si, the differences in $(3/2)\lambda_{100}$ between the current and previous work are associated with the differences in thermal treatments, as both the short-range ordering (SRO) (Ref. 12) and phase mixture[11,12,13] are dependent on thermal processing.

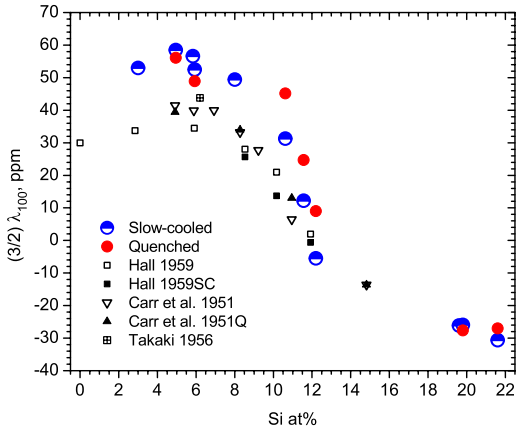

FIG. 1. (Color online) Dependence of magnetostriction on composition and thermal processing. Slow-cooled: 10 °C/min from 1000 °C. Quenched: ice-water quenched from 1000 °C. Hall 1959: cooling-chamber cool. Hall1959SC: 1.2 °C/h. Carr *et al.* 1951: 50–100 °C/h. Carr *et al.* 1951Q: oil quenched from 900 °C. Takaki 1956: Bridgman-grown at 10 mm/min.

The change in $(3/2)\lambda_{100}$ correlates with the regions of the phase diagram,[14] revealing that the magnetostriction is phase dependent. In the single phase A2 region up to ~10 at. % Si, $(3/2)\lambda_{100}$ is positive, with a maximum about 59 ppm at 5 at. % Si. In the single phase $D0_3$ region between ~15 and ~25 at. % Si, the constant is negative, with a minimum about −31 ppm at 21.6 at. % Si. The (100) superlattice peak in XRD spectra for an Fe-21.6 at. % Si is sharp, giving a full width at half maximum (FWHM) for 2θ at about 0.1°, consistent with a fully ordered $D0_3$ phase. Between 10 and 15 at. % Si, it is likely that phase mixtures involving A2, B2, and $D0_3$ are present, depending on thermal processing. Therefore, a rule of mixture may control the strain value within this composition range, causing $(3/2)\lambda_{100}$ to change from positive to negative as has been found in Fe–Ge alloys.[7] At a faster cooling rate a larger portion of high temperature phase A2 or/and B2 is believed to be retained, consequently resulting in larger differences in magnetostrictive strain between quenched and slow-cooled alloys. The role of B2 structure playing in the magnetostrictive behavior is not clear and is under investigation.

Examining the single phase A2 region (up to ~10 at. % Si from the phase diagram) more closely, $(3/2)\lambda_{100}$ reaches a maximum and then decreases. This behavior is distinctly different from the magnetostrictive behaviors of Fe–Ga,[1] Fe–Al,[4] and Fe–Ge[7] single crystals. Recent studies revealed the occurrence of B2 and $D0_3$ SRO in the Fe–Si alloys between 5 and 8 at. % Si.[15–17] The magnetostriction decrease within the A2 regime is very likely to be associated with the formation of SRO. To confirm this link, XRD was performed on a slow-cooled sample of 8 at. % Si (Fig. 2). A SRO peak for (100) superlattice scattering at $2\theta=31.6°$ with a FWHM of 2.52°, was calculated by fitting with Gaussian function. Using Scherrer's formula,[18] the SRO length scale was estimated to be 3.4 nm. As the ordered $D0_3$ phase shows negative magnetostriction and SRO is the precursor of long-range ordering, it is reasonable to expect the formation of $D0_3$ SRO will lead to reductions in magnetostriction.

A magnetostriction constant is determined by magneto-

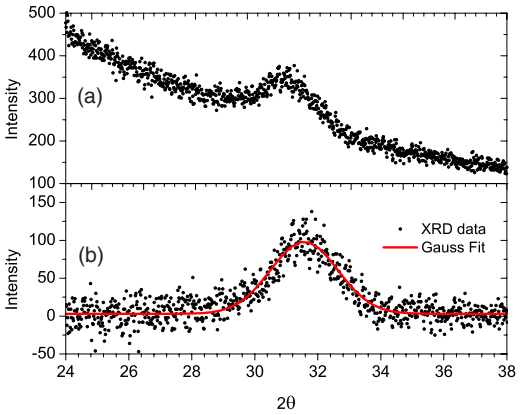

FIG. 2. (Color online) XRD peak showing the SRO in a slow-cooled Fe-8 at. % Si: (a) original data and (b) after background subtraction and Gaussian fitting.

elastic coupling factor and shear modulus for a material. As the shear modulus is a mechanical property, it is helpful to understand the magnetism by knowing the coupling factor. The comparison of magnetoelastic coupling factors of the Fe-based alloys is shown in Fig. 3, in light of the published data.[4,8,19–23] It is clear that Fe–Si alloys show smaller coupling factors than those of Fe–Ga and Fe–Ge alloys.

IV. SUMMARY

The magnetostriction constant, $(3/2)\lambda_{100}$, of Fe–Si single crystals was measured via a strain gauge method. XRD was employed in SRO study and phase identification. $(3/2)\lambda_{100}$ was found to be phase dependent: it showed positive strains in the single phase A2 regime and negative strains in the single phase $D0_3$ regime, and changed from positive to negative between the two regimes. SRO in the A2 regime decreased $(3/2)\lambda_{100}$ from a maximum value at ~5 at. % Si. In the single phase regimes of A2 and $D0_3$, thermal history had negligible effects on $(3/2)\lambda_{100}$. In the regions of phase mixture involving A2, B2, and $D0_3$ phases, quenching shifted the change in $(3/2)\lambda_{100}$ from positive to negative to higher Si contents.

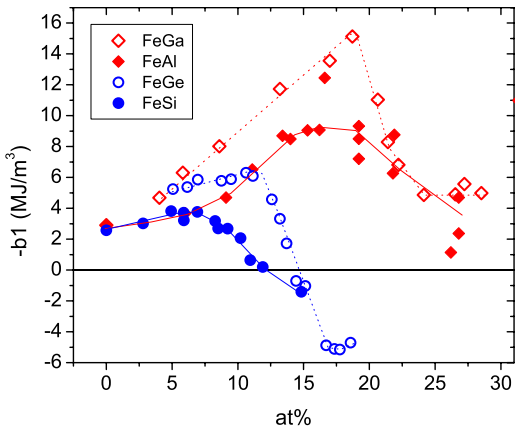

FIG. 3. (Color online) Comparison of coupling factors, $-b1$, among Fe–Ga, Fe–Al, Fe–Ge, and Fe–Si alloys. Fe–Ga and Fe–Al data are from Ref. 4, Fe–Ge data are from Ref. 7, and Fe–Si data are calculated from Refs. 5, 9, and 19–23. $-b1=3/2\lambda_{100}(c_{11}-c_{12})$, where c_{11} and c_{12} are elastic constants. Lines are drawn to guide the eyes.

ACKNOWLEDGMENTS

The authors thank W. M. Yuhasz for comments on this paper. This work was supported by the U.S. Department of Energy, Office of Basic Energy Sciences, Division of Materials Sciences. The research was performed at the Ames Laboratory. Ames Laboratory is operated for the U.S. Department of Energy by Iowa State University under Contract No. DE-AC02-07CH11358.

[1]Q. Xing, Y. Du, R. M. McQueeney, and T. A. Lograsso, Acta Mater. **56**, 4536 (2008).
[2]Q. Xing and T. A. Lograsso, Appl. Phys. Lett. **93**, 182501 (2008).
[3]E. M. Summers, T. A. Lograsso, and M. Wun-Fogle, J. Mater. Sci. **42**, 9582 (2007).
[4]A. E. Clark, J. B. Restorff, M. Wun-Fogle, D. Wu, and T. A. Lograsso, J. Appl. Phys. **103**, 07B310 (2008).
[5]R. C. Hall, J. Appl. Phys. **30**, 816 (1959).
[6]O. Ikeda, I. Ohnuma, R. Kainuma, and K. Ishida, Intermetallics **9**, 755 (2001).
[7]D. Wu, Q. Xing, R. W. McCallum, and T. A. Lograsso, J. Appl. Phys. **103**, 07B307 (2008).
[8]G. Petculescu, J. B. LeBlanc, M. Wun-Fogle, J. B. Restorff, W. M. Yuhasz, T. A. Lograsso, and A. E. Clark, J. Appl. Phys. **105**, 07A932 (2009).
[9]W. J. Carr, Jr., and R. Smoluchowski, Phys. Rev. **83**, 1236 (1951).
[10]H. Takaki and T. Tsuji, J. Phys. Soc. Jpn. **11**, 1153 (1956)
[11]R. Gersdorf, "On magnetostriction of single crystals of iron and some dilute iron alloys," Ph.D. thesis, University of Amsterdam, 1961.
[12]S. Matsumura, H. Oyama, and K. Oki, Mater. Trans., JIM **30**, 695 (1989).
[13]K. Raviprasad and K. Chattopadhyay, Acta Metall. Mater. **41**, 609 (1993).
[14]*Binary Alloy Phase Diagrams*, 2nd ed., edited by T. B. Massalski (ASM International, Materials Park, OH, 1990).
[15]N. V. Ershov, Yu. P. Chernenkov, V. A. Lukshina, and V. I. Fedorov, Phys. Solid State **51**, 441 (2009).
[16]Yu. P. Chernenkov, N. V. Ershov, V. A. Lukshina, V. I. Fedorov, and B. K. Sokolov, Physica B **396**, 220 (2007).
[17]N. V. Ershov, V. A. Lukshina, B. K. Sokolov, Yu. P. Chernenkov, and V. I. Fedorov, J. Magn. Magn. Mater. **300**, e469 (2006).
[18]B. D. Culity, *Elements of X-ray Diffraction* (Addision-Wesley, New York, 1956), p. 259.
[19]J. A. Rayne and B. S. Chandrasekhar, Phys. Rev. **122**, 1714 (1961).
[20]A. E. Lord and D. N. Beshers, J. Appl. Phys. **36**, 1620 (1965).
[21]J. L. Routbort, C. N. Reid, E. S. Fisher, and D. J. Dever, Acta Metall. **19**, 1307 (1971).
[22]H. L. Alberts and P. T. Wedepohl, Physica **53**, 571 (1971).
[23]A. Machova and S. Kadeckova, Czech. J. Phys., Sect. B **27**, 555 (1977).